

Vacuum Beam Guide for Large Scale Quantum Networks

Yuexun Huang,^{1,*} Francisco Salces – Carcoba,² Rana X Adhikari,² Amir H. Safavi-Naeini,³ and Liang Jiang^{1,†}

¹*Pritzker School of Molecular Engineering, University of Chicago, Chicago, Illinois 60637, USA*

²*Division of Physics, Math, and Astronomy, LIGO Laboratory,
California Institute of Technology, Pasadena, CA 91125 USA*

³*Department of Applied Physics and Ginzton Laboratory, Stanford University, Stanford, CA 94305 USA*

(Dated: December 25, 2023)

The vacuum beam guide (VBG) presents a completely different solution for quantum channels to overcome the limitations of existing fiber and satellite technologies for long-distance quantum communication. With an array of aligned lenses spaced kilometers apart, the VBG offers ultra-high transparency over a wide range of optical wavelengths. With realistic parameters, the VBG can outperform the best fiber by three orders of magnitude in terms of attenuation rate. Consequently, the VBG can enable long-range quantum communication over thousands of kilometers with quantum channel capacity beyond 10^{13} qubit/sec, orders of magnitude higher than the state-of-the-art quantum satellite communication rate. Remarkably, without relying on quantum repeaters, the VBG can provide a ground-based, low-loss, high-bandwidth quantum channel that enables novel distributed quantum information applications for computing, communication, and sensing.

It is an outstanding challenge to build an effective low-loss quantum channel for global-scale quantum networks, which will enable transformative applications of secure quantum communication [1], distributed quantum sensing [2], and network-based quantum computation [3, 4]. The main obstacle is the absorption loss of optical channels, with attenuation length limited to tens of kilometers for fiber and free-space channels, resulting in an exponential decrease in the direct quantum communication rate over long distances. Significant progress has been made in extending the communication distances for quantum networks, including satellite-based quantum entanglement distribution over 1200 km [5] and memory-enhanced quantum communication [6] beyond the repeater-less bounds [7, 8]. However, satellite-based quantum channels are fragile, expensive, and restricted by local weather conditions [9, 10]. Furthermore, quantum repeaters without full quantum error correction will still suffer from a polynomial decrease in communication rate over long distances [11]. Hence, it is highly desirable to establish a reliable quantum channel capable of directly transmitting quantum signals over vast distances, such as the continental scale of 10^4 km (with an attenuation rate of at the level of 10^{-4} dB/km) for a wide range of optical frequencies.

To overcome this challenge, we explore a completely different approach – the vacuum beam guide (VBG) — which uses an array of lenses (in an evacuated tube) to guide light, as opposed to relying on total reflection induced by fiber. The large vacuum spacing between lenses significantly reduces the effective travel length of light in optical materials, thus eliminating the problem of material absorption. Inspired by quantum communication satellites, the VBG channel is set up within a vacuum

chamber tube, which eliminates air absorption and effectively isolates the channel from the outer environment, ensuring robustness against environmental perturbations. Although beam waveguides were proposed for classical optical communication [12], it was taken over by low-cost optical fiber, which is sufficient for classical communication, despite its intrinsic loss. For quantum communication, however, it is crucial that the design of the vacuum beam guide has the potential to achieve ultra-low-loss long-distance communication. With the ability to build large-scale vacuum chambers hosting precision optical elements separated by multiple kilometers, we can make exciting scientific discoveries, such as gravitational wave detection by the Laser Interferometer Gravitational-wave Observatory (LIGO) [13].

Here, we propose deploying the VBG as the backbone quantum channel toward a global quantum network with a hierarchy structure as shown in Fig. 1(a-b). We model the system and estimate the upper bound of the attenuation dominated by residue air absorption, optical losses introduced by lenses, and misalignment of the beam guide. Our estimation demonstrates the VBG as state-of-the-art under a practical and exemplifying configuration, establishing it as one of the most practical and potentially useful quantum communication techniques at a global scale.

Ultra-High Transmission of VBG. The VBG is a long vacuum chamber tube that consists of an array of N_{tot} lenses spaced L_0 apart, which enables the connection of quantum terminals separated by $L_{\text{tot}} = N_{\text{tot}}L_0$, as illustrated in Fig. 1(c). The vacuum has a typical pressure below ~ 1 Pascal, which ensures low absorption from the remaining gas at room temperature. The lenses are shielded from seismic vibrations and are optically aligned with adaptive feedback. In this analysis, we consider a feasible and robust confocal design with a spacing of $L_0 = 4$ km and a focal length of $f = L_0/2$. The beam waist is $w_0 = \sqrt{\lambda f/\pi} \approx 3$ cm for the telecom-band wavelength λ . The lens radius of $R = 10$ cm is sufficient to

* yesunhuang@uchicago.edu

† liang.jiang@uchicago.edu

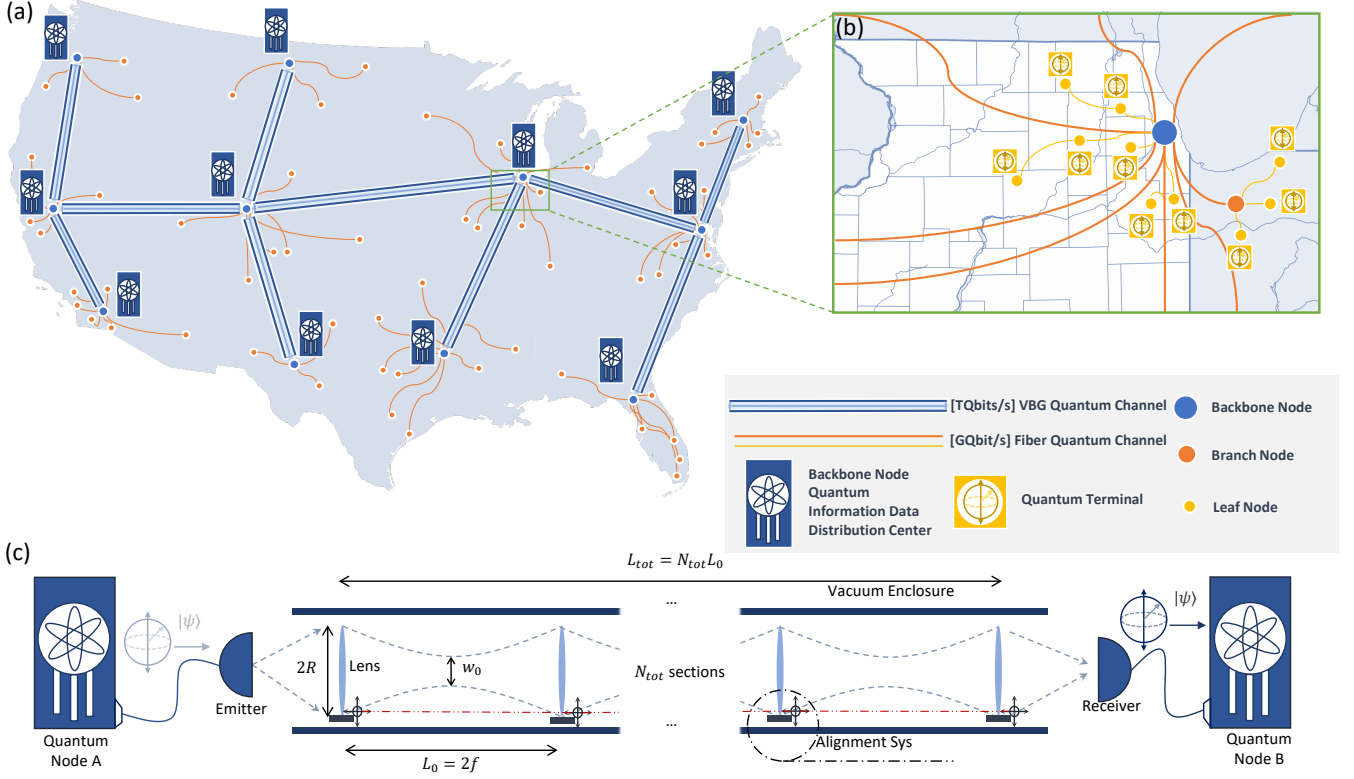


FIG. 1. A hierarchical structure of large-scale quantum networks connected by vacuum beam guides (VBGs). (a) The VBG backbone network (blue links) can transfer quantum information with high capacity (with TeraQubits/sec) over long distances, connecting regional quantum networks (orange links). (b) The regional network consists of fiber or free-space quantum channels designed to distribute quantum information to branch nodes and quantum terminals (with GigaQubits/sec) across urban scales. (c) The design of the VBG involves placing lenses with identical focus length f and radius R at regular intervals within a vacuum chamber tube, constructing a VBG with N_{tot} sections. The positions of the lenses are stabilized by an advanced alignment system. In the VBG, the fundamental Gaussian mode with waist w_0 can travel at an extremely low loss over a distance of L_{tot} . Quantum states can be transferred from quantum node A at one end of the VBG to quantum node B at the other end of the VBG.

achieve negligible diffraction loss.

Optical signals encoding quantum information can transmit through the VBG with little loss, even after passing through an array of aligned lenses over thousands of kilometers. The effective attenuation rate (in units of dB/km) characterizes the VBG transmission loss, with three major contributions associated with the lens, residual gas, and imperfect alignment:

$$\alpha_{tot} = \alpha_{lens} + \alpha_{gas} + \alpha_{align}. \quad (1)$$

We now discuss the conditions to achieve an attenuation rate at the level of 10^{-4} dB/km for all three contributions.

The lens loss, α_{lens} , is associated with absorption, scattering, reflection, and diffraction. As illustrated in Fig. 2(a), a lens radius of $R \geq 10$ cm is adequate to suppress diffraction loss for $L_0 = 4$ km. Furthermore, by adding a multi-layer anti-reflective coating, the total loss per lens can be reduced to less than 10^{-4} , resulting in an effective loss rate of $\alpha_{lens} < 10^{-4}$ dB/km at the wavelengths $\lambda \approx 1550$ nm, which can match the telecom band

[16].

Gas loss in the VBG is primarily due to the absorption from residual air in the vacuum chamber tube. As shown in Fig. 2(b), we compute the attenuation rate α_{gas} at various levels of gas pressure with the components of air based on the HITRAN database [17]. At a pressure of 1 Pascal, the attenuation rate is $\alpha_{gas} < 10^{-4}$ dB/km for optical wavelengths within the selected telecom bands. Further reducing the air pressure below 10^{-2} Pascal is sufficient to achieve negligible air absorption by reducing attenuation rate below 10^{-4} dB/km almost over the entire spectrum.

We can derive an upper bound for the effective attenuation rate induced by imperfect alignment in the confocal design:

$$\alpha_{align} \leq -\frac{10}{L_0} \log_{10} \left[1 - \frac{2\sigma_s^2}{w_0^2} - \frac{\sigma_{L_0}^2}{L_0^2} - \frac{\sigma_f^2}{f^2} \right], \quad (2)$$

where σ_s and σ_{L_0} are the magnitudes of the fluctuations of transverse and longitudinal displacements for

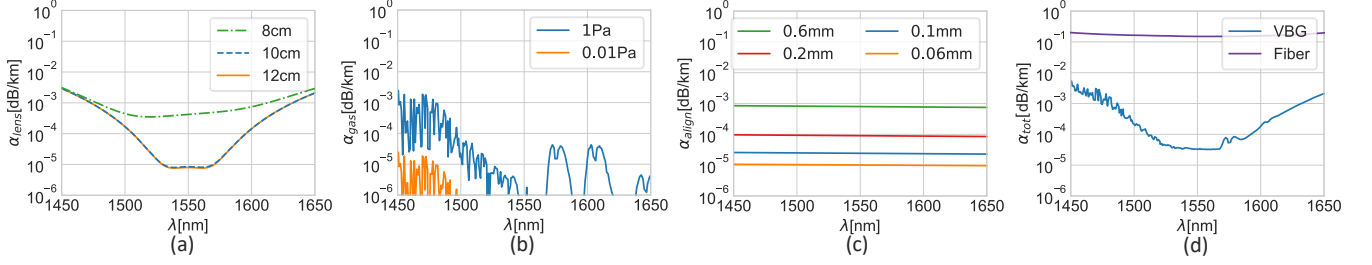


FIG. 2. Different effective attenuation rates as a function of wavelength under various configurations. (a) Attenuation rate from the lenses, α_{lens} , with lens radius $R = 8, 10, 20$ cm. For a large radius ($R \geq 10$ cm), the lens loss is limited by residual reflection and absorption from the AR coating. (b) Attenuation rate due to residual gas, α_{gas} , with moderate vacuum pressures: $P = 0.01, 1$ Pa. (c) The misalignment attenuation rate, α_{align} , with random transverse displacements $\sigma_s = 0.06, 0.1, 0.2, 0.6$ mm while fixing $\frac{\sigma_{L_0}}{L_0} = \frac{\sigma_f}{f} = 0.1\%$. (d) The total attenuation rate of the VBG compared to the advanced fiber [14, 15] under the configuration of $L_0 = 4$ km, $R = 10$ cm, $P = 1$ Pascal, and $\sigma_s = 0.1$ mm.

each lens, and σ_f is the deviation of the focal length. The general bound for α_{align} for near confocal design is derived in Supplementary Material [16]. Since $w_0 \ll L_0, f$, the fluctuating transverse displacement is the dominant cause of attenuation, while the other two contributions can be sufficiently small, $\frac{\sigma_{L_0}}{L_0}, \frac{\sigma_f}{f} < 10^{-3}$, achievable with current technology [16]. As illustrated in Fig. 2(c), it is essential to have good transverse alignment (e.g., $\sigma_s < 0.2$ mm) to achieve a low effective attenuation rate ($\alpha_{\text{align}} < 10^{-4}$ dB/km). Even with relatively poor alignment (e.g., $\sigma_s = 0.6$ mm), we can still achieve $\alpha_{\text{align}} < 10^{-2}$ dB/km, which is much better than the attenuation rate of fiber by at least an order of magnitude. Practically, each lens will be actively positioned using slow actuators, based on standard alignment sensing systems [18], bringing the residual mis-centering to < 0.1 mm.

By summing up all three contributions, we can plot the total attenuation rate along with the individual contributions in Fig. 2(d), assuming practical parameters such as $R = 10$ cm, $P = 1$ Pascal, and $\sigma_s = 0.1$ mm. The VBG can achieve an attenuation level as low as 5×10^{-5} dB/km for an optimized choice of wavelength within the atmospheric window, which corresponds to an effective attenuation length of 80,000 km, more than three orders of magnitude better than state-of-the-art fiber technology.

Quantum Channel Capacities of VBG. We can use the VBG as a highly transparent bosonic quantum channel to transmit quantum information over long distances [19]. The VBG has a transmission efficiency at wavelength λ

$$\eta[\lambda] = 10^{-0.1 L_{\text{tot}} \alpha[\lambda]}, \quad (3)$$

which can be used for various quantum communication protocols. For one-way quantum communication (e.g., from Alice to Bob only), the one-way pure-loss capacity

for a single wave packet at a wavelength λ is given by

$$q_1[\lambda] = \max \left[\log_2 \left(\frac{\eta[\lambda]}{1 - \eta[\lambda]} \right), 0 \right], \quad (4)$$

which vanishes for $\eta[\lambda] \leq 1/2$. If the pure-loss VBG channel is further assisted by two-way classical communication (between Alice and Bob), the corresponding two-way pure-loss capacity at a wavelength λ is [20]

$$q_2[\lambda] = \log_2 \left(\frac{1}{1 - \eta[\lambda]} \right). \quad (5)$$

which is finite for all $\eta[\lambda] > 0$.

As shown in the insets of Fig. 3, the VBG can have a broad band with a large one-way or two-way channel capacity over long distances. In the low-loss regime with $L_{\text{tot}} \ll 1/\alpha$, efficient multi-mode encoding techniques can be used to approach the asymptotic scaling of one-way channel capacity [21].

We can calculate the frequency-integrated channel capacity, which provides the maximum transmission rate of quantum information, by integrating over the frequency [22]:

$$Q_{1(\text{or}2)} \equiv \int q_{1(\text{or}2)} d\nu = \int q_{1(\text{or}2)}[\lambda] \frac{c}{\lambda^2} d\lambda, \quad (6)$$

for one-way and two-way quantum communication protocols, respectively. The VBG has a significant advantage over other techniques, particularly due to its ultra-low attenuation rate over a wide range of wavelengths, leading to an extremely large quantum capacity exceeding 10^{13} qubits/second over a distance of 10^4 km under one-way quantum communication protocol as shown in Fig. 3(a). While the estimation in Fig. 3(b) suggests that even with a baseline coupling loss as large as 50%, where the one-way protocol fails, it is still possible to achieve a Tera-level qubit rate via two-way protocols for continental scale communication. This points out a practically feasible pathway toward ultra-fast global quantum networks.

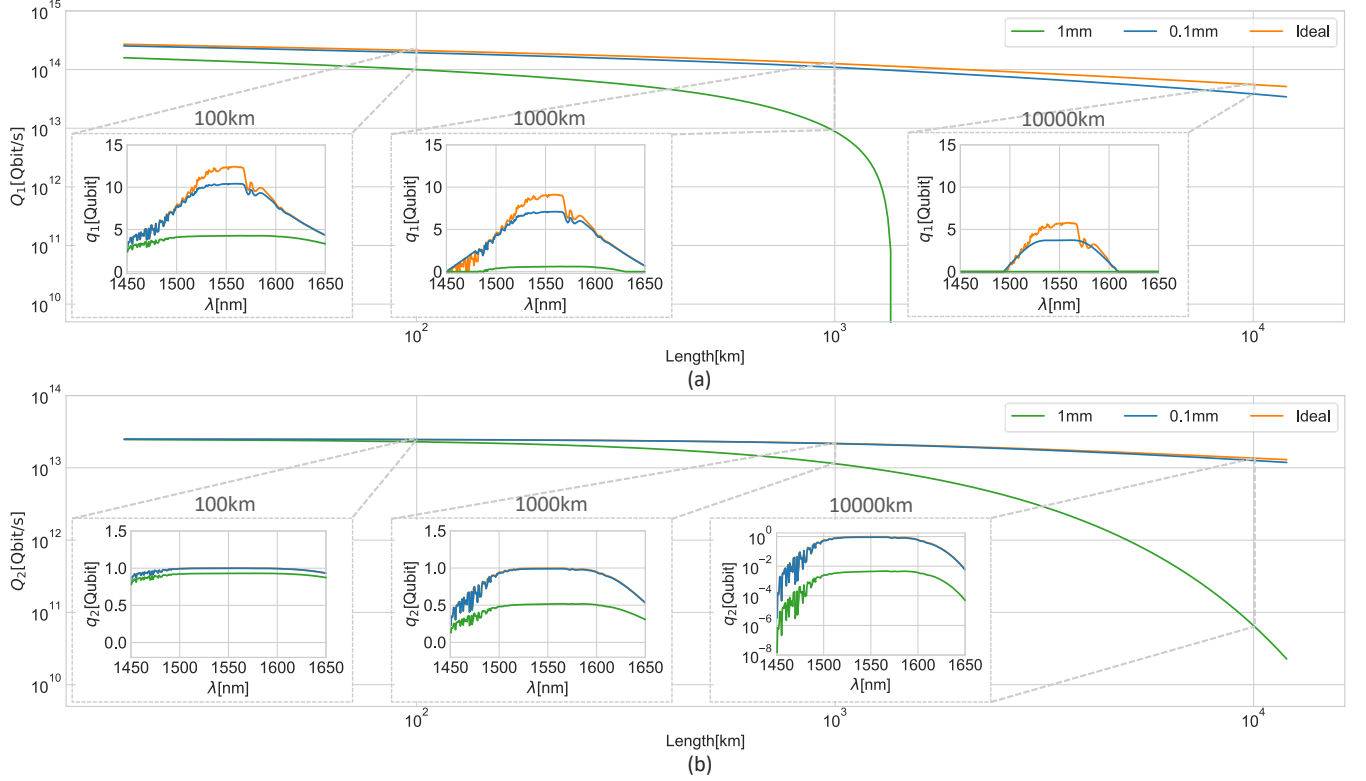


FIG. 3. The quantum channel capacity $Q_{1(or2)}$ at 1 Pascal as a function of transmission distance with $\sigma_s = 0.1$, 1 mm when fixing $\frac{\sigma_{L0}}{L_0} = \frac{\sigma_f}{f} = 0.1\%$ compared to the ideal alignment. (a) One-way frequency-integrated quantum capacity with perfect coupling. (b) Two-way frequency-integrated quantum capacity assuming 50% coupling efficiency. The insets show the relation between channel capacity $q_{1(or2)}$ as a function of wavelength at $L = 100, 1000, 10000$ km. The inset of 10000 km in (b) is in log scale to show finite two-way quantum capacity over a wide range of parameters.

Compared to state-of-the-art satellite-ground links for quantum communication [23], the ground-based VBG offers high reliability as it is operational at all times, and provides an extremely high throughput, at least eight orders of magnitude higher in terms of achievable quantum communication rate. The concept of a beam guide [12] was investigated to address diffraction loss in satellite-relayed quantum communication [10]. Nevertheless, that protocol remains susceptible to atmospheric and turbulence-induced losses, thereby affecting reliability, transmission rate, channel capacity, and communication latency (due to the limitation of two-way quantum communication). Additionally, unlike quantum repeaters [24], the VBG only requires passive optical lenses to focus the optical beams and does not need any quantum memory or active quantum devices to perform quantum error detection or correction. Therefore, the VBG should be feasible to implement with current technology.

Discussion. We can also design the VBG to operate with visible light, which would benefit from a larger air transmission window and low-loss lens materials if sufficiently small lens roughness is achievable, while better transversal alignment is required to match the reduced beam waist $w_0 \propto \lambda^{1/2}$ with shorter wavelengths. In

practice, there will be a trade-off between the VBG's performance and cost, and we can optimize its design parameters to achieve the desired balance.

Summary and Outlook. We have presented a ground-based VBG scheme that enables the implementation of a highly transparent and reliable optical quantum channel with an effective attenuation length of over 10^4 km and a large communication bandwidth. With currently available technology, the VBG can establish a continuous quantum channel connecting remote quantum devices with an ultra-high quantum capacity above 10^{13} qubits/second over continental scales, orders of magnitude higher than other approaches using satellites and quantum repeaters.

By addressing the challenge of lossy quantum channels, our high-throughput VBG has the potential to revolutionize quantum networks, enabling a wide range of exciting novel quantum network applications, such as global-scale secure quantum communication [1], ultra-long-based optical telescopes [2], quantum network of clocks [25], quantum data centers [26], and delegated quantum computing [27, 28].

Acknowledgments We thank David Awschalom, Saikat Guha, Dan Brown, Ming Lai, John Preskill

and Peter Zoller for helpful comments and discussions. We acknowledge support from the ARO(W911NF-23-1-0077), ARO MURI (W911NF-21-1-0325), AFOSR MURI (FA9550-19-1-0399, FA9550-21-1-0209, FA9550-23-1-0338), NSF (PHY-0823459, PHY-1764464, ECCS-1941826, OMA-1936118, ERC-1941583, OMA-2137642,

OSI-2326767, CCF-2312755), NTT Research, Packard Foundation (2020-71479), and the Marshall and Arlene Bennett Family Research Program. This material is based upon work supported by the U.S. Department of Energy, Office of Science, National Quantum Information Science Research Centers.

-
- [1] F. Xu, X. Ma, Q. Zhang, H.-K. Lo, and J.-W. Pan, Secure quantum key distribution with realistic devices, *Reviews of Modern Physics* **92**, 025002 (2020).
- [2] D. Gottesman, T. Jennewein, and S. Croke, Longer-baseline telescopes using quantum repeaters, *Physical Review Letters* **109**, 070503 (2012).
- [3] H. J. Kimble, The quantum internet, *Nature* **453**, 1023 (2008).
- [4] S. Wehner, D. Elkouss, and R. Hanson, Quantum internet: A vision for the road ahead, *Science* **362**, eaam9288 (2018).
- [5] J. Yin, Y. Cao, Y.-H. Li, S.-K. Liao, L. Zhang, J.-G. Ren, W.-Q. Cai, W.-Y. Liu, B. Li, H. Dai, G.-B. Li, Q.-M. Lu, Y.-H. Gong, Y. Xu, S.-L. Li, F.-Z. Li, Y.-Y. Yin, Z.-Q. Jiang, M. Li, J.-J. Jia, G. Ren, D. He, Y.-L. Zhou, X.-X. Zhang, N. Wang, X. Chang, Z.-C. Zhu, N.-L. Liu, Y.-A. Chen, C.-Y. Lu, R. Shu, C.-Z. Peng, J.-Y. Wang, and J.-W. Pan, Satellite-based entanglement distribution over 1200 kilometers, *Science* **356**, 1140 (2017).
- [6] M. K. Bhaskar, B. Riedinger, B. Machielse, D. S. Levonian, C. T. Nguyen, E. N. Knall, H. Park, D. Englund, M. Lončar, D. D. Sukachev, and M. D. Lukin, Experimental demonstration of memory-enhanced quantum communication, *Nature* **580**, 60 (2020).
- [7] M. Takeoka, S. Guha, and M. M. Wilde, Fundamental rate-loss tradeoff for optical quantum key distribution, *Nat Commun* **5**, 10.1038/ncomms6235 (2014).
- [8] S. Pirandola, R. Laurenza, C. Ottaviani, and L. Banchi, The ultimate rate of quantum cryptography, arXiv:1510.08863 (2015).
- [9] S.-K. Liao, W.-Q. Cai, W.-Y. Liu, L. Zhang, Y. Li, J.-G. Ren, J. Yin, Q. Shen, Y. Cao, Z.-P. Li, F.-Z. Li, X.-W. Chen, L.-H. Sun, J.-J. Jia, J.-C. Wu, X.-J. Jiang, J.-F. Wang, Y.-M. Huang, Q. Wang, Y.-L. Zhou, L. Deng, T. Xi, L. Ma, T. Hu, Q. Zhang, Y.-A. Chen, N.-L. Liu, X.-B. Wang, Z.-C. Zhu, C.-Y. Lu, R. Shu, C.-Z. Peng, J.-Y. Wang, and J.-W. Pan, Satellite-to-ground quantum key distribution, *Nature* **549**, 43 (2017).
- [10] S. Goswami and S. Dhara, Satellite-relayed global quantum communication without quantum memory, *Physical Review Applied* **20** (2023).
- [11] S. Muralidharan, L. Li, J. Kim, N. Lütkenhaus, M. D. Lukin, and L. Jiang, Optimal architectures for long distance quantum communication, *Scientific Reports* **6**, 20463 (2016).
- [12] G. Goubau, Beam waveguides, *Advances in Microwaves* **3**, 67 (1968).
- [13] B. P. Abbott *et al.*, Observation of gravitational waves from a binary black hole merger, *Physical Review Letters* **116**, 061102 (2016).
- [14] M. Kakui, M. Matsui, T. Saitoh, and Y. Chigusa, Ultra-low-loss (0.1484 db/km) pure silica core fibre and extension of transmission distance, *Electronics Letters* **38**, 1 (2002).
- [15] H. Sakr, T. D. Bradley, G. T. Jasion, E. N. Fokoua, S. R. Sandoghchi, I. A. Davidson, A. Taranta, G. Guerra, W. Shere, Y. Chen, *et al.*, Hollow core nanfs with five nested tubes and record low loss at 850, 1060, 1300 and 1625nm, in *Optical Fiber Communication Conference* (Optica Publishing Group, 2021) pp. F3A–4.
- [16] See Supplemental Material at URL-will-be-inserted-by-publisher for the details of derivation.
- [17] R. V. Kochanov, I. Gordon, L. Rothman, P. Wcisło, C. Hill, and J. Wilzewski, Hitran application programming interface (hapi): A comprehensive approach to working with spectroscopic data, *Journal of Quantitative Spectroscopy and Radiative Transfer* **177**, 15 (2016).
- [18] K. L. Dooley, L. Barsotti, R. X. Adhikari, M. Evans, T. T. Fricke, P. Fritschel, V. Frolov, K. Kawabe, and N. Smith-Lefebvre, Angular control of optical cavities in a radiation-pressure-dominated regime: the enhanced ligo case, *J. Opt. Soc. Am. A* **30**, 2618 (2013).
- [19] A. S. Holevo and R. F. Werner, Evaluating capacities of bosonic gaussian channels, *Physical Review A* **63**, 032312 (2001).
- [20] S. Pirandola, R. Laurenza, C. Ottaviani, and L. Banchi, Fundamental limits of repeaterless quantum communications, *Nature communications* **8**, 15043 (2017).
- [21] K. Noh, V. V. Albert, and L. Jiang, Improved quantum capacity bounds of gaussian loss channels and achievable rates with gottesman-kitaev-preskill codes, *IEEE Transactions on Information Theory* **65**, 2563 (2019).
- [22] C.-H. Wang, F. Li, and L. Jiang, Quantum capacities of transducers, *Nature Communications* **13**, 6698 (2022).
- [23] Y.-A. Chen, Q. Zhang, T.-Y. Chen, W.-Q. Cai, S.-K. Liao, J. Zhang, K. Chen, J. Yin, J.-G. Ren, Z. Chen, S.-L. Han, Q. Yu, K. Liang, F. Zhou, X. Yuan, M.-S. Zhao, T.-Y. Wang, X. Jiang, L. Zhang, W.-Y. Liu, Y. Li, Q. Shen, Y. Cao, C.-Y. Lu, R. Shu, J.-Y. Wang, L. Li, N.-L. Liu, F. Xu, X.-B. Wang, C.-Z. Peng, and J.-W. Pan, An integrated space-to-ground quantum communication network over 4,600 kilometres, *Nature* **589**, 214 (2021).
- [24] K. Azuma, S. E. Economou, D. Elkouss, P. Hilaire, L. Jiang, H.-K. Lo, and I. Tzitrin, Quantum repeaters: From quantum networks to the quantum internet, arXiv:2212.10820 (2022).
- [25] P. Komar, E. M. Kessler, M. Bishof, L. Jiang, A. S. Sorensen, J. Ye, and M. D. Lukin, A quantum network of clocks, *Nat Phys* **10**, 582 (2014).
- [26] J. Liu, C. T. Hann, and L. Jiang, Quantum data center: Theories and applications, arXiv: 2207.14336 (2022).
- [27] S. Barz, E. Kashefi, A. Broadbent, J. F. Fitzsimons, A. Zeilinger, and P. Walther, Demonstration of blind quantum computing, *science* **335**, 303 (2012).
- [28] J. F. Fitzsimons, Private quantum computation: an introduction to blind quantum computing and related pro-

ocols, [npj Quantum Information](#) **3**, 23 (2017).